NMEI 27

MASTER

New Mexico Energy Institute

at New Mexico State University

ENHANCED HEAT EXTRACTION FROM HOT-DRY-ROCK GEOTHERMAL RESERVOIRS DUE TO INTERACTING SECONDARY THERMAL CRACKS

FINAL REPORT

This research was conducted with the support of the New Mexico Energy and Minerals Department (EMD) and the New Mexico Energy Institute at New Mexico State University (NMEI-NMSU) under Contract EMD-77-2113. However, any opinions, findings, conclusions, or recommendations expressed within this report are those of the authors and do not necessarily reflect the views of EMD or NMEI-NMSU.

NMEI 27

DISCLAIMER

ENHANCED HEAT EXTRACTION FROM HOT-DRY-ROCK GEOTHERMAL RESERVOIRS DUE TO INTERACTING SECONDARY THERMAL CRACKS

Final Report
(2/1/78-1/31/79)

Principal Investigator
Y. C. Hsu, Ph.D.
Department of Mechanical Engineering
The University of New Mexico
Albuquerque, New Mexico 87131

by

Y. C. Hsu, Ph.D.
Y. M. Lu
Department of Mechanical Engineering
The University of New Mexico

NMEI 27

April 1979

ACKNOWLEDGEMENTS

We would like to thank Dr. R. L. San Martin and Ms. Arlene Starkey for their encouragement and support concerning this investigation, and Bureau of Engineering Research, Ms. Margo Otero and Mrs. Jan Smith for typing and editing this report.

ABSTRACT

The potential for enhanced heat extraction or power production for a hot-dry-rock (HDR) reservoir (sometimes even for the low-temperature-hot water reservoir) due to the increased heat transfer surface area resulting from these thermal secondary cracks is of significant importance to the project. These cracks, afforded by cooling-induced stresses in the rock adjacent to the main (primary) hydraulically-formed fracture surfaces, may represent the most effective means of reservoir enlargement.

The formation and growth of such thermal secondary cracks was being studied in a more realistic analytical representation. What we have investigated is on how the circulating fluid (or water) through the main hydraulic fracture and the thermally-induced secondary, growing, interacting cracks affects the time-varying temperature, deformations, stresses, thermal crack geometry, water flow rates through the main and thermal cracks, $\dot{Q}_m$ and $\dot{Q}_{t.c.}$, reservoir coolant outlet temperature, T, and reservoir thermal power, $\dot{E}$, of the cracked geothermal reservoir. This problem was dealt with in the presence of the interaction of fluid, solid reservoir, or rock and energy. The coupled partial differential equations, which are formulated based on conservation of mass, linear momentum and energy, were solved in conjunction with fracture mechanics. In other words, the contribution of these thermal cracks with time to the above-mentioned overall reservoir thermal performance was investigated.

Even fluid and rock temperatures were obtained for growing, interacting cracks, however, the value of K_I used here was still obtained based on a single thermal crack perpendicular to the rock surface within the framework of a two-dimensional assumption. In other words, K_I used here was not accounted for by these growing, interacting cracks. Since the value of K_I for a single thermal crack is smaller than the one for multiple thermal cracks, K_{Im}, K_{Im} would reach to K_{Ic} earlier than K_I does. As such, K_{Im} would generate larger crack geometry at a particular time. So, the time-varying crack geometry, $\dot{Q}_m$ and $\dot{Q}_{t.c.}$, T and $\dot{E}$, obtained based on K_I is smaller and on the conservative side, compared

with ones obtained based on K_{lm}. Finding K_{lm} will be carried out in the Phase 2 period.

Calculations are carried out for the LASL Fenton Hill HDR-Reservoir with H = 100 m, W = 70 m, t = 0.2 m, h = 2.6 km, $\dot{Q}$ = 230 gpm, θ_o = 50°C, T_r = 180°C, $\mu = 1.4 \times 10^{-4}$ Pa-sec and rock properties (see Table 1). Three equally-spaced edge cracks are initiated at ten days with d = 1.5 m, s = 1.34 m, w = 0.05 mm and ℓ = 5 m. For the small size main fracture system and with relatively low initial rock temperatues, the significant effect of thermal stress cracking is to flatten due to the temperature drawdown at later times. Even though the thermal power is more than doubled at 180 days, this occurs at an outlet reservoir temperature of only 81°C (see Figure 12). In Figure 12, at 60 days for a constant flow rate of 230 gpm, the thermal drawdown curve with thermal stress cracking is only about 12°C above that without thermal stress cracking (85.9°C versus 73.5°C). It would appear that the effects of thermal stress cracking in this reservoir could easily be increased by several inadvertent shutdowns, changes in flow rate and by inferring a slightly larger effective heat transfer area for the reservoir.

Calculations can also be applied to the low-temperature-hot water reservoir.

TABLE OF CONTENTS

LIST OF FIGURES

LIST OF TABLES

NOMENCLATURE

$A(y)$	the area of the main (primary) hydraulic crack (on one side) swept by the water in transversing from 0 to y
A_t	the total area of the main hydraulic crack (rectangular crack, on one side)
c	the specific heat of water
c_r	the specific heat of rock
d, d_i	the depth of secondary thermal cracks and the crack group denoted by i
E_r	Young's modulus of rock
$\dot{E}$	reservoir thermal power
h	the depth between the earth's surface and the center of the main, hydraulic fracture
H	the length of the main hydraulic crack
K_1	the stress-intensity factor of the opening mode
K_{1c}	critical K_1 or the fracture toughness
K_{1m}	a value of K_1 for multiple thermal cracks
ℓ	the length of secondary thermal cracks
p	the pressure of water
p_o	the water pressure at inlet of the main, hydraulic crack
$\dot{Q}$	volumetric flow rate of water through the reservoir
$\dot{Q}_m$	volumetric flow rate of water through the main, hydraulic crack
$\dot{Q}_{t.c.}$	volumetric flow rate of water through secondary thermal cracks
s	the spacing of the secondary thermal cracks
t	the opening width of the main, hydraulic crack

NOMENCLATURE (continued)

T	the temperature of rock or the reservoir coolant outlet temperature
T_o	the tensile strength of rock
T_r	the initial rock temperature
v_y	the velocity of water through the main, hydraulic crack
v_{yi}	the velocity of water through a thermal crack denoted by i
w, w_i	the width of the opening of secondary thermal cracks and the crack group denoted by i
W	the width of the main, hydraulic crack
x	the horizontal coordinate in the fracture plane
y	the vertical coordinate in the fracture plane
z	a coordinate orthogonal to the fracture plane
α_r	thermal diffusivity of rock
Δy	a finite length in y-coordinate
θ	water temperature
θ_o	the water inlet temperature of reservoir
θ_{out}	the water outlet temperature of reservoir
λ	thermal conductivity of water
λ_r	thermal conductivity of rock
μ	viscosity of water
ν_r	Poisson's ratio of rock
ρ	density of water
ρ_r	density of rock
σ_{xx}	the maximum horizontal earth principal stress
σ_{yy}	the overburden earth pressure (or the maximum compressive principal stress)
σ_{zz}	the minimum horizontal earth principal stress

CHAPTER 1

INTRODUCTION

The potential for enhanced heat extraction or power production for a hot-dry-rock (HDR) reservoir (sometimes even for the low-temperature-hot water reservoir) due to the increased heat transfer surface area resulting from these thermal secondary cracks is of significant importance to the project. These cracks, afforded by cooling-induced stresses in the rock adjacent to the main (primary) hydraulically-formed fracture surfaces, may represent the most effective means of reservoir enlargement.

The results in [1][1] of the New Mexico Energy Research and Development supported (NMER&D) project show that the heat extraction from the geothermal reservoir can be increased only about 25-30 percent by means of thermal secondary noninteracting cracks in a state of equilibrium. In order to improve further the heat extraction process, the above-mentioned two restrictions which are underlined must be removed to consider the thermal secondary, continuously growing, interacting cracks. Both the increased heat transfer surface area opened by thermal secondary cracks, and the total amount of heat available to the circulating fluid (water) would increase as the energy is withdrawn from the reservoir and the thermal

---

[1] Numbers in brackets designate references at end of the report.

secondary interacting cracks continuously grow. To this end, the proposed research work must concentrate to further increase the heat extraction from the HDR reservoir (and sometimes even from the low-temperature-hot water reservoir as reported in [1]) of such thermal secondary, continuously growing, interacting cracks. The HDR reservoir is mainly used for generating electricity, in addition to high-temperature chemical process, space heating and air conditioning. The low-temperature-hot water reservoir is used for low-temperature chemical process, space heating and air conditioning.

For this project, the formation and growth of such thermal secondary cracks was being studied in a more realistic analytical representation. What we have investigated is on how the circulating fluid (or water) through the main hydraulic fracture and the thermally-induced secondary, growing, interacting cracks affects the time-varying temperature, deformations, stresses, thermal crack geometry, water flow rates through the main and thermal cracks, $\dot{Q}_m$ and $\dot{Q}_{t.c.}$, reservoir coolant outlet temperature, T, and reservoir thermal power, $\dot{E}$, of the cracked geothermal reservoir. This problem was dealt with in the presence of the interaction of fluid, solid reservoir, or rock and energy. The coupled partial differential equations, which are formulated based on conservation of mass, linear momentum and energy, were solved in conjunction with fracture mechanics. In other words, the contribution of these thermal cracks with time to the above-mentioned overall reservoir thermal performance was investigated.

Even fluid and rock temperatures were obtained for growing, interacting cracks, however, the value of K_1 used here was still obtained based on a single thermal crack perpendicular to the rock surface within the framework of a two-dimensional assumption. In other words, K_1 used here was not accounted for by these growing, interacting cracks. Since the value of K_1 for a single thermal crack is smaller than the one for multiple thermal cracks, K_{1m}, K_{1m} would reach to K_{1c} earlier than K_1 does. As such, K_{1m} would generate larger crack geometry at a particular time. So, the time-varying crack geometry, $\dot{Q}_m$ and $\dot{Q}_{t.c.}$, T and $\dot{E}$, obtained based on K_1 is smaller and on the conservative side, compared with ones obtained based on K_{1m}.

In Chapter 1, the introduction of this investigation was described. In Chapter 2, the simplified version of the proposed hot-dry-rock geothermal reservoir is considered. In Chapter 3, a closed-form solution of the rock temperature without thermal crack was found and substituted into SAP-IV computer code to calculate the stresses. These stresses being superposed with earth stresses and fluid pressure were used in conjunction with the fracture mechanics criterion to determine the initiation of secondary thermal crack. After the initiation of secondary thermal crack, the rock temperature was then calculated by a two-dimensional heat conduction program, "AYER". In Chapter 4, the detailed procedures for carrying out steps mentioned in Chapter 3 were listed. In Chapter 5, solutions developed in Chapters 2 through 4 were applied to study the time-varying temperature field, thermal stresses and

crack geometry produced, and additional heat power generated in the reservoir. In Chapter 6, conclusions were discussed and summarized.

CHAPTER 2

STATEMENT OF THE PROBLEM

A simplified main fracture geometry in Figure 1 has been selected which is similar to that inferred from the initial stages of reservoir drawdown during the 75-day Heat Extraction Experiment at Los Alamos Scientific Laboratory (LASL). This simplified model is further idealized as a vertical, rectangular crack (Figure 2) with its total effective heat transfer area A_t (one side). The crack opening, t, is of constant thickness. The rock is initially at T_r. Cold water is injected at inlet y = 0, with inlet temperature θ_o and a hot water outlet is at the top. The crack opening, t, is small (~ 0.2 mm) while height, H, and width, W, of the reservoir are large (~ 100 m).

Of investigation is to study how the circulating fluid (water) in the main hydraulic crack and these resulting secondary thermal cracks interact to affect the temperature distribution, the stresses, the thermal crack geometry, $\dot{Q}_m$, $\dot{Q}_{t.c}$, $\dot{E}$ and the reservoir coolant outlet temperature of the cracked geothermal reservoir. This problem will be investigated by simultaneously considering the interactions between the flowing fluid, reservoir rock, and energy extraction process, as set forth in two steps in Chapter 3.

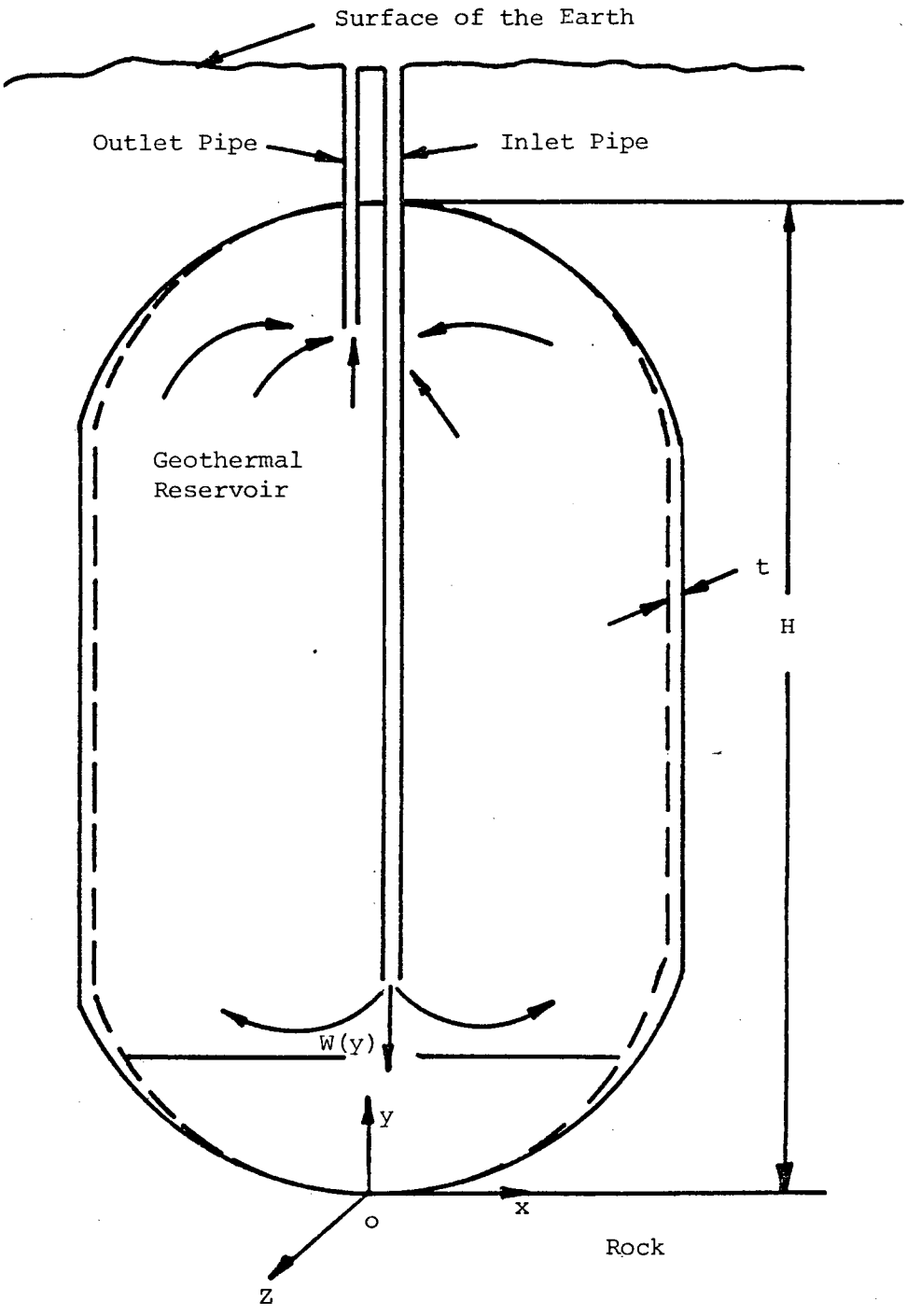

Figure 1. Proposed hot-dry-rock geothermal reservoir

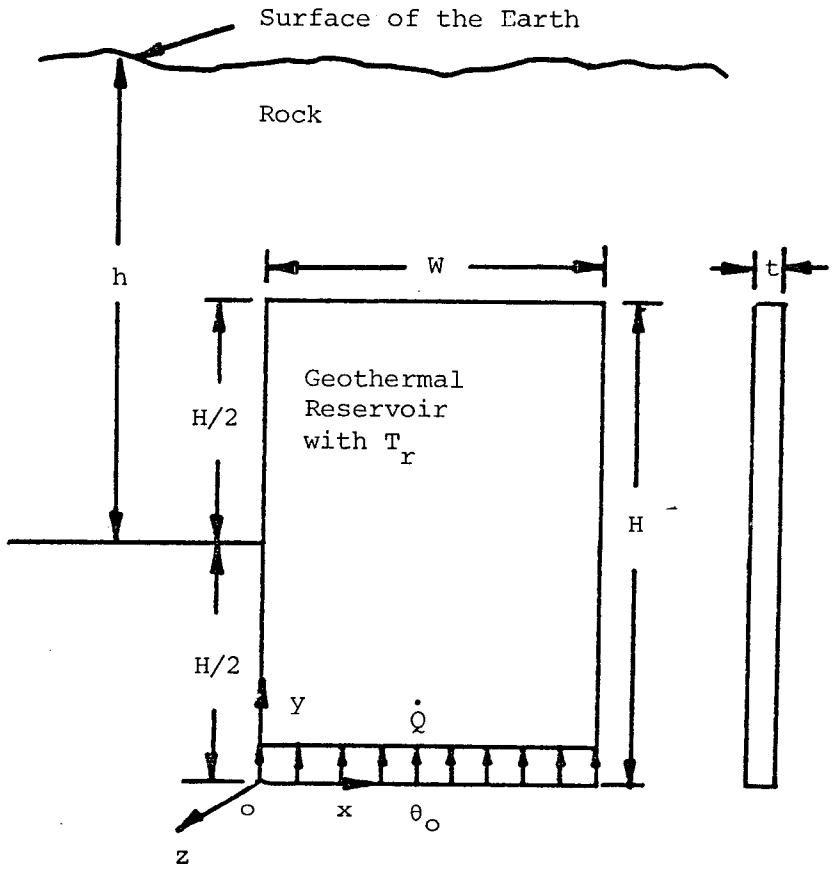

Figure 2. Simplified version of the proposed hot-dry-rock geothermal reservoir

CHAPTER 3

TWO STEPS ON HOW TO ATTACK THE PROBLEM

3.1 Step 1 - Before Any Secondary Thermal Crack is Initiated

Figure 2 shows the hydraulically fractured, main geothermal reservoir in the absence of any secondary thermal crack. Since the working fluid is single-phase water, it is assumed to be incompressible. Since this fluid is, further, entirely confined to the crack between assumed impermeable rock surface, heat is transferred to this fluid only by thermal conduction through the solid rock surfaces.

The constant velocity of the flow along the y-coordinate, v_y, is:

$$v_y = \dot{Q}/Wt \tag{1}$$

where W and $\dot{Q}$ are the width of the main hydraulic crack and the total flow rate in the absence of any secondary thermal crack.

For Hager-Poisewille flow in the reservoir, v_y is [2]:

$$v_y = -\frac{1}{12}\frac{t^2}{\mu}\left(\frac{\partial p}{\partial y}\right) \tag{2}$$

where μ and p are viscosity and pressure distribution of the fluid. Rewrite (2) as:

$$\frac{\partial p}{\partial y} = -\frac{12\mu v_y}{t^2} \tag{3}$$

Integrating (3) with the boundary condition of $p = p_o$ at $y = 0$, the resulting form is:

$$p(y) = p_o - \frac{12\mu v_y}{t^2} y \quad . \tag{4}$$

The actual geometry of the hot-dry rock geothermal reservoir (crack) is arbitrary but both A_t and t may be a function of x and y (see Figure 1 representing the proposed geothermal reservoir). Here, the crack opening, t, is small (~ 0.2 mm) while height, H, and width, W, of the reservoir are large (~ 100 m). Cold water is injected at inlet, y = 0, with inlet temperature, θ_o. Define A(y) as the area of reservoir (on one side) at any position of y = y which is swept by the fluid traveling from y = 0 to y = y.

Since t is small, fluid properties are independent of the z-coordinate. Since heat fluxes in the z-coordinate are so small, the fluid temperature, θ, assumes to be equal to the rock surface temperature. Further, fluid properties are averaged with respect to x-coordinate. As such, the proposed problem is reduced to the problem with transient rock conduction in the z-coordinate and transient fluid convection in the y-coordinate. The corresponding rock and fluid energy equations, boundary, and initial conditions reduce to:

rock energy equation

$$\frac{\partial^2 T}{\partial z^2} = \frac{1}{\alpha_r} \frac{\partial T}{\partial \tau} \quad , \tag{5}$$

fluid energy equation by neglective storage

$$\rho c \dot{Q} \frac{\partial \theta}{\partial y} = 2\lambda_r W(y) \left.\frac{\partial T}{\partial z}\right|_{z=0} \quad , \tag{6}$$

boundary conditions

$$\theta(y,\tau) = T(y,z = 0,\tau) \ , \tag{7}$$

$$\theta(0,\tau) = \theta_o \ , \tag{8}$$

$$T(y,z \to \infty,\tau) = T_r \ , \tag{9}$$

initial condition

$$T(y,z,\tau = 0) = T_r \ , \tag{10}$$

By using Laplace transformation, solutions of T and θ in (5) and (6) can be obtained subject to (7) and (10). Rock temperature distribution $T(y,z,\tau)$ was obtained by Hugh Murphy [3] at LASA to be

$$T(y,z,\tau) = \theta_o + (T_r - \theta_o) \ \text{erf} \left[\{z/2 + \lambda_r A(y)/\rho c \dot{Q}\} \Big/ \sqrt{\alpha_r \tau} \right] \tag{11}$$

where

$$A(y) = \int_o^y W(u)du \ . \tag{12}$$

For simplicity, Figure 2 will be used to approximate Figure 1. As such, all the calculations will be carried out based on Figure 2. The stresses in rock were then calculated by substituting the fluid pressure in (4) and the rock temperature in (11) into the SAP-IV computer code [4]. These stresses were used in conjunction with the fracture mechanics criterion in order to determine the initiation of any secondary thermal crack [1].

3.2 Step 2 - After the Initiation of Secondary Thermal Cracks

As secondary thermal cracks in Figure 3 form with the above-obtained initial values of depth d, opening w, and length ℓ, we

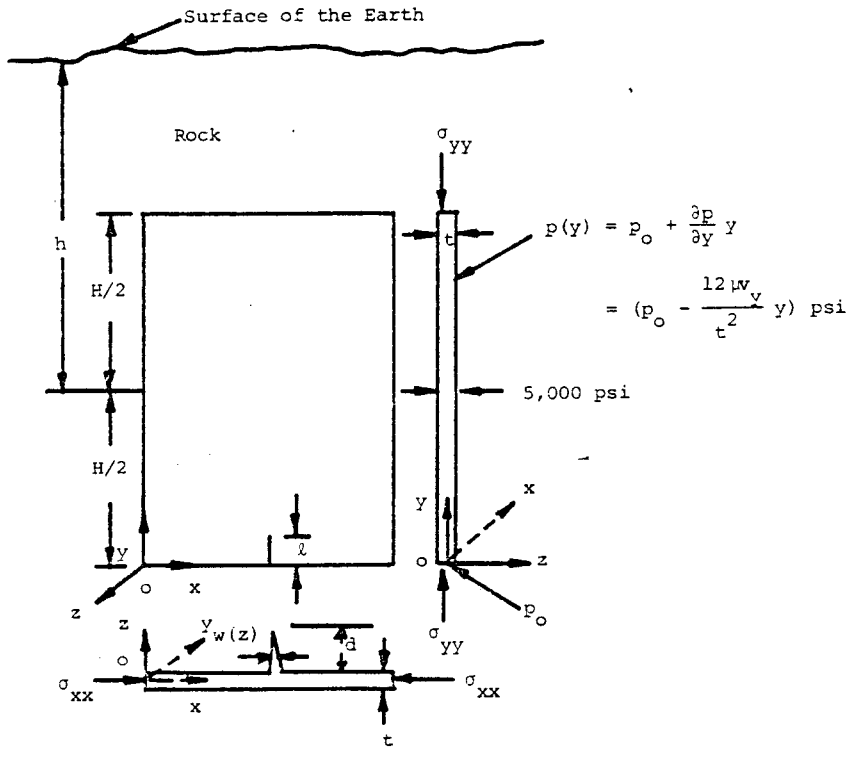

Figure 3. The initiation of secondary thermal cracks on the surface of a geothermal reservoir

start to consider the effects of secondary thermal cracks. We subdivided the main hydraulic crack into ten equally spaced strips along the y-coordinate (see Figure 3). For each strip, we solved a two-dimensional heat conduction problem in the presence of second thermal cracks and calculated rock temperature. The corresponding thermal stresses and the geometry of thermal cracks in the cracked (thermally) rock will be investigated by implementing cracks into the SAP-IV computer code.

CHAPTER 4

PROCEDURES FOR CARRYING OUT TWO STEPS

The detailed procedures for carrying out steps 1 and 2 are listed as follows:

(a) To calculate the fluid (water) velocity, $v_{yi}(z)$, through each thermal crack denoted by i, from (2),

$$v_{yi}(z) = -\frac{1}{12}\frac{w_i^2(z)}{\mu}\left(\frac{\partial p}{\partial y}\right)_i \tag{13}$$

(b) To calculate the total flow rate through n thermal cracks,

$$\dot{Q}_{t.c.} = \sum_{i=1}^{n}\int_{o}^{d_i} v_{yi}(z)w_i(z)\,dz\ . \tag{14}$$

(c) To calculate the new flow rate through the main hydraulic crack, $\dot{Q}_m$ as:

$$\dot{Q}_m = \dot{Q} - \dot{Q}_{t.c.}\ , \tag{15}$$

where $\dot{Q}_{t.c.}$ is represented in (14).

(d) To calculate new velocity by substituting $\dot{Q}_m$ in (15) into (1).

(e) To calculate new pressure by substituting the above-mentioned new velocity into (4).

(f) To obtain the rock surface temperature on the main hydraulic crack, $T(y,z=0,\tau)$, from (11) by taking z = 0.

(g) To derive the surface temperature of thermal cracks based on the principle of energy balance at the interface between the fluid (water) and the rock surface of the secondary thermal cracks, as shown in Figure 4. At a given value of x, one has

$$v_y(z)w(z)\,\frac{\partial\theta(y,z)}{\partial y} = -\,2\lambda_r\,\frac{\partial T(y,z)}{\partial x}\ ,$$

which yields the water temperature

$$\theta(y,z) = -\,\frac{2\lambda_r}{v_y(z)w(z)}\int_o^y \frac{\partial T(y,z)}{\partial x}\,dy\ . \tag{16}$$

For a single element in Figure 4b, the surface temperature of the thermal crack, $T(y,z)$, is then

$$T(y,z) \cong \theta(y,z)$$

$$= -\,\frac{2\lambda_r}{v_y(z)w(z)}\,\frac{\partial T}{\partial x}\,(\Delta y)\ , \tag{17}$$

where $v_y(z)$ is represented in (13).

(h) To calculate the rock temperature in the presence of thermal cracks by using the surface temperature on the main hydraulic crack (procedure (f)) and thermal cracks (procedure (g)), the initial temperature and two-dimensional heat conduction code, AYER in [5], which was developed by Robert Lawton at LASL. In addition, the heat flux through the surfaces of the main hydraulic crack and secondary thermal cracks can also be calculated.

(i) To calculate new thermal stresses and the corresponding spacing, opening, depth, and length of these new thermal cracks by using the new rock temperature obtained in procedure (h).

(j) To go back to procedure (a).

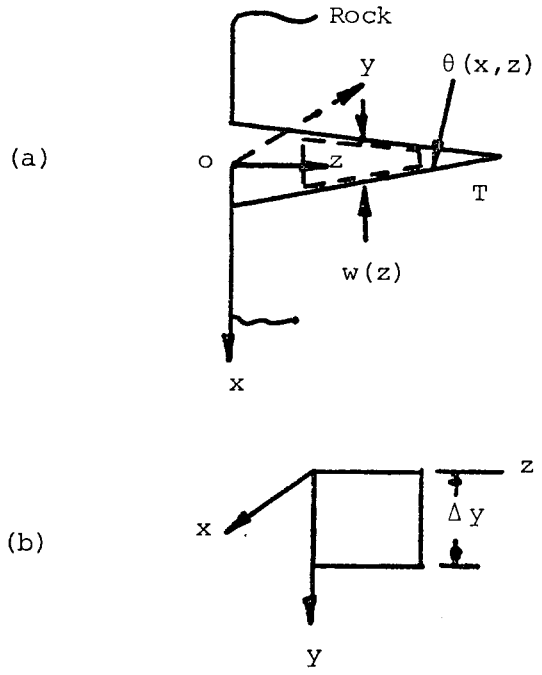

Figure 4. Sketch of a single thermal crack at a given value of x

CHAPTER 5

APPLICATIONS TO GEOTHERMAL RESERVOIRS

5.1 Description of Geothermal Reservoir

For the LASL Fenton Hill reservoir in Figure 2, H = 100 m, W = 70 m, t = 0.2 mm, h = 2.6 km, $\dot{Q}$ = 230 gpm, θ_o = 50°C, and T_r = 180°C. The physical properties of rock used are listed in Table 1. The fluid used is water and its viscosity, μ, is equal to 1.4×10^{-4} Pa-sec. The corresponding form of (11) becomes

$$T(y,z,\tau) = 50 + 130 \text{ erf } [(1.701\, z + 1.254 \times 10^{-2}\, y)/\sqrt{\tau}]\,°C\,. \tag{18}$$

Physical Properties	Values
conductivity, λ_r	2.9 watt/m-K
density, ρ_r	2700 kg/m^3
heat capacity, c_r	1000 J/kg-K
thermal diffusivity, α_r	1.07×10^{-6} m^2/sec
Young's modulus, E_r	4×10^5 bars
Poisson's ratio, ν_r	0.22
tensile strength, T_o	80 bars

Table 1. Physical properties of rock

5.2 A Finite Element Model of Geothermal Reservoir

For modeling the problem of the simplified version of the proposed Hot-Dry-Rock geothermal reservoir, the half symmetry part of a vertical rectangular crack with its surroundings is represented

by a solid of geometrical form of a rectangular parallelepiped of which the dimension lengths in the x-, y-, and z-directions are 50 m, 120 m, and 16 m, respectively, as shown in Figure 5. In order to choose the dimension of the length in the z-direction, we used (18) to calculate the penetration depth due to the cooling effect of the flowing water through the major crack at the time period of one year. An approximate result of 16 m was then determined.

Figure 5 shows the finite elements used to represent the rectangular parallelepiped. The 390 node points and 240 thick-shell finite elements are arranged. However, the region of interest is bounded by the head line, where the temperature field, the thermal stress field, and the generated secondary thermal cracks are considered.

5.3 Results Obtained Before Any Secondary Thermal Crack is Initiated

Using the above mentioned $T(y,z,\tau)$ obtained from (18) as the input to the above-chosen thick-shell element, the thermal stresses of the rock were calculated for different time periods by using the SAP IV codes.

In addition to the thermal stresses produced by the cooling of the rock, the overburden pressure σ_{yy} and the horizontal earth stresses, σ_{xx} and σ_{zz}, of the rock and the water pressure (see Figure 3) are also considered for calculating the principal stresses and their corresponding principal directions. The values of

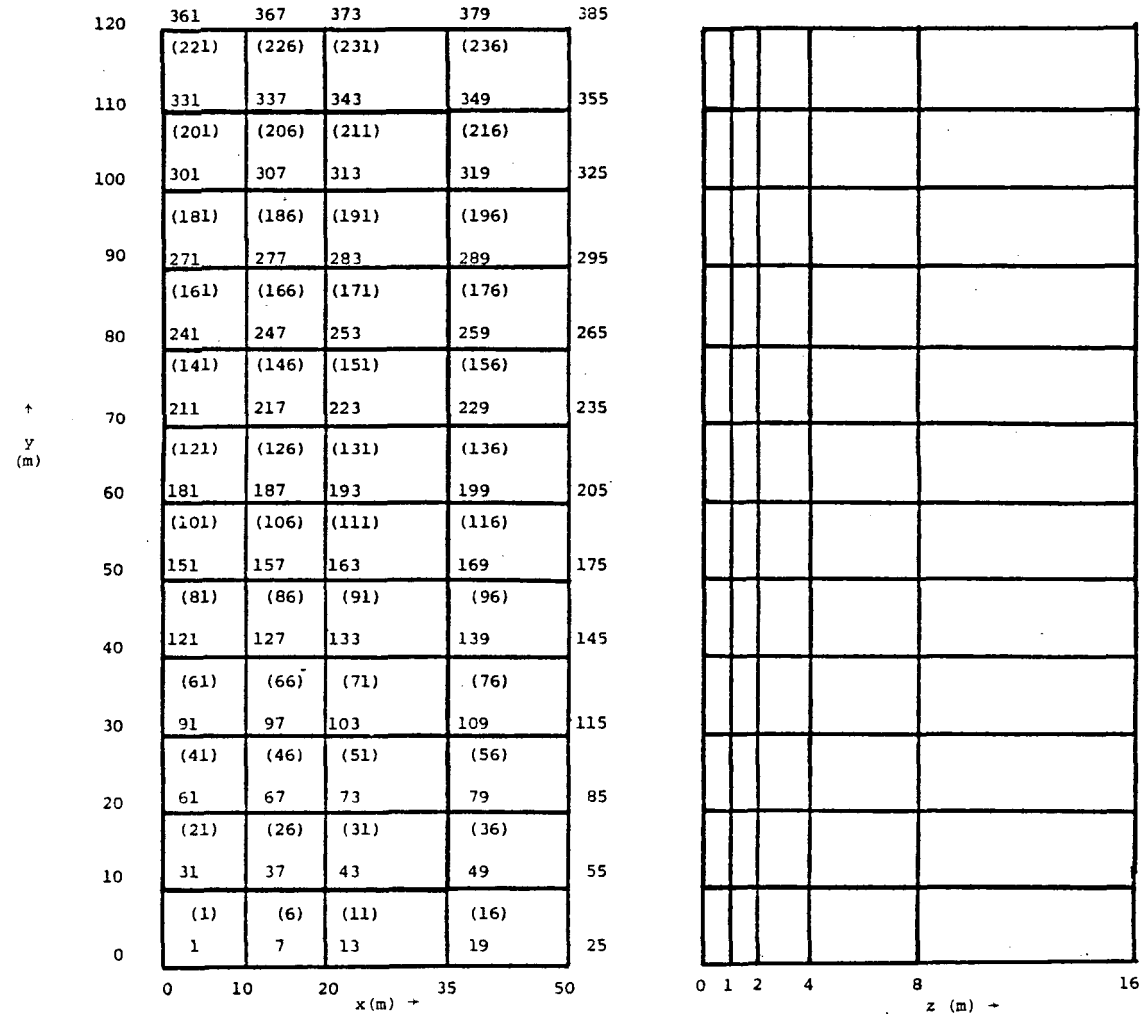

Figure 5. Finite element discretizations for half of the rectangular crack (390 node points and 240 thick-shell finite elements)

p_o = 4,600 psi, σ_{xx} = 5,000 psi, σ_{yy} = 10,000 psi, and σ_{zz} = 5,000 psi will be used for the above mentioned calculations.

The secondary thermal cracks are predicted based upon principal stresses, their principal directions, and fracture mechanics by using a computer program for computing depth, spacing and opening of these secondary thermal cracks.

By using the above-mentioned data, it was calculated that three equally-spaced thermal cracks have been produced at an inlet of cold water and the center of the main hydraulic crack (see Figure 6) after ten days of reservoir operating time. The depth, the spacing, the opening and the length of these initially thermal cracks were calculated to be d = 1.5 m, s = 1.34 m, w = 0.05 mm, and ℓ = 5 m.

5.4 Results Obtained After the Initiation of Secondary Thermal Cracks (S.T.C.)

Having investigated the temperature field without the S.T.C. for time periods ranging from ten days to one year, we found that the temperature gradient along the z-direction is much larger than that along the y-direction. After the initiation of the S.T.C. at ten days, the problem is converted to the one with a transient rock conduction in both the z-direction and x-direction, and with a transient fluid convection in the y-direction. As such, a 2-D problem is assumed. Divide the rectangular parallelepiped into ten strips by cutting along the x-z plane and solve the temperature fields of each strip by using the "AYER" heat conduction program. Here, the general two dimensional transient equation of

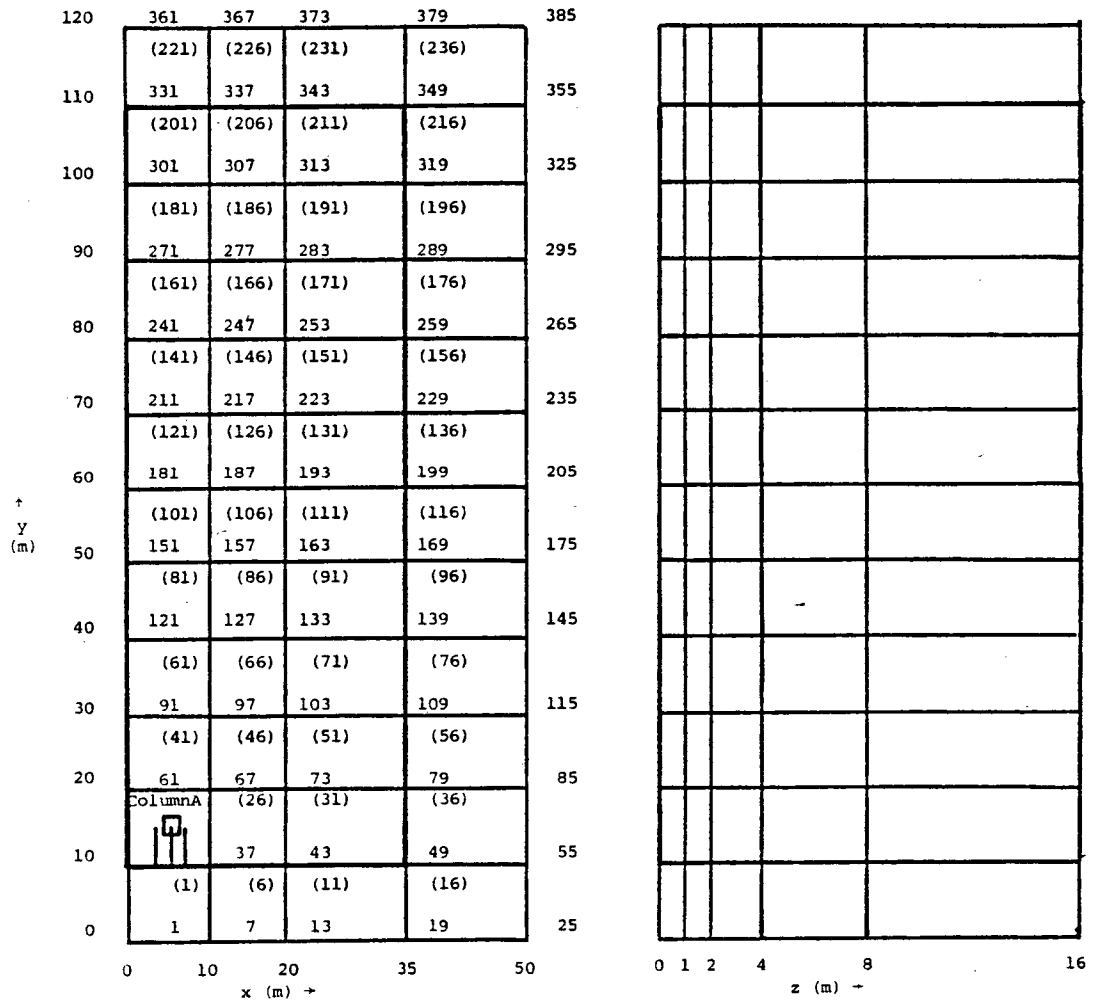

Figure 6. Three equally-spaced edge cracks (d = 1.5 m, s = 1.34 m, w = 0.05 mm and ℓ = 5 m) at time step of ten days

heat conduction was solved by considering the convective heat transfer due to the fluid flowing through the complicated boundary.

Much time was spent in converting the "AYER" code in the CDC-version to the IBM-version. As time goes on, the secondary thermal cracks vary in size and the geometry input of the "AYER" code gets more complicated (see Figure 7). As such, the input subroutine was modified to improve the efficiency of the "AYER" code. By using this code, results were run on an IBM machine. These results agree well with results obtained from the CDC machine.

In order to see the interacting effects due to the circulating water through the secondary thermal cracks, we have set up two models, one without these cracks (w/o S.T.C.) and the other with these cracks (w/S.T.C.). The temperature fields, the thermal stresses, the geometry of secondary thermal cracks, the outlet temperature of fluid, and the power were calculated for the above-mentioned two models after 20 days, 30 days, 2 months, 3 months, 6 months, and 1 year of reservoir operating time. The results are listed in Table 2 and plotted in Figures 8 through 12.

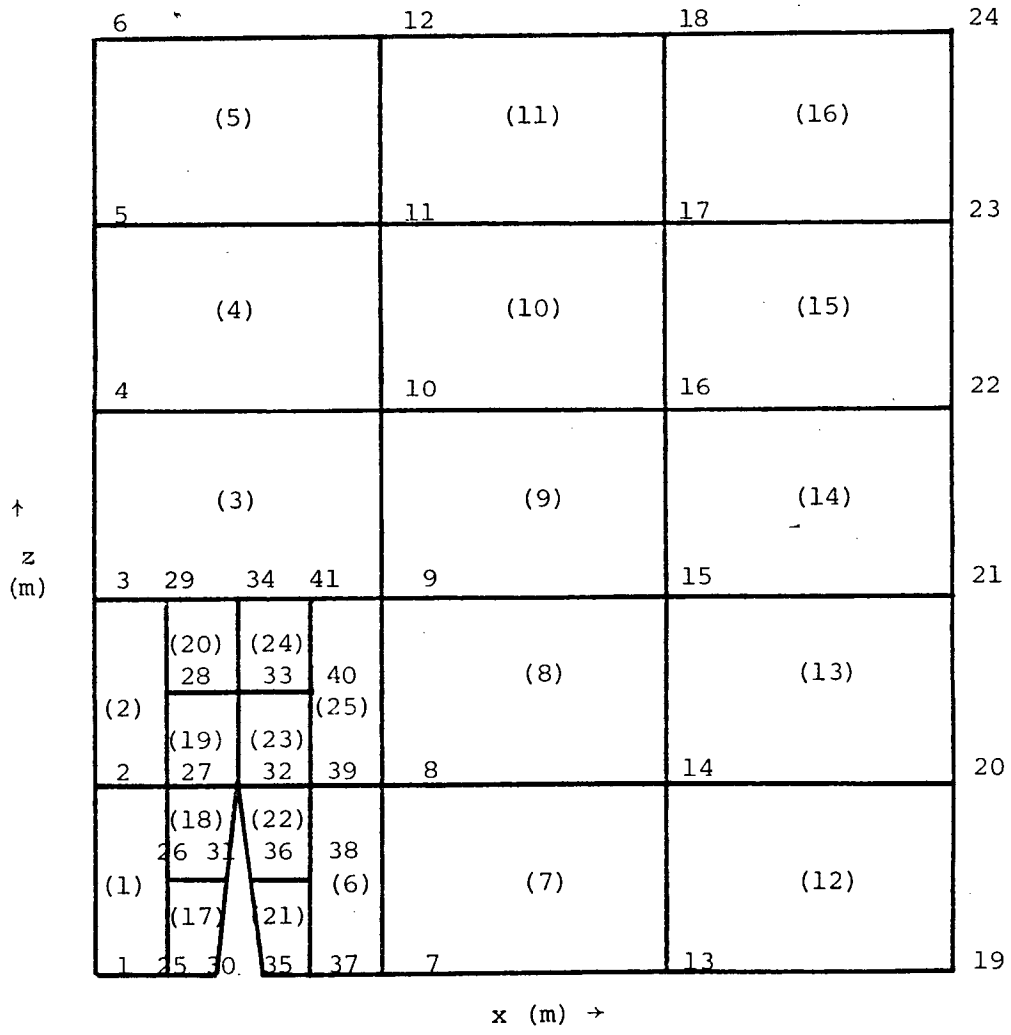

Figure 7 Mesh discretizations through a strip of rock with a single edge crack

Time (days)	d(m)	s(m)	ℓ(m)	w(mm)	θ_{out}^{*}(°C)	$\dot{E}$(MW)
10	1.50	1.34	5	0.05	105.3	3.22
20	1.89	1.53	35	0.06	90.1	2.33
30	2.17	1.66	55	0.07	83.0	1.92
60	2.86	1.93	70	0.10	73.5	1.37
90	3.20	2.16	85	0.13	69.3	1.12
180	4.80	2.56	95	0.20	63.7	0.80
360	7.71	3.74	100	0.29	59.7	0.56
10	1.50	1.34	5	0.05	107.2	3.33
20	2.44	2.19	55	0.08	96.2	2.69
30	2.81	2.16	75	0.09	92.8	2.49
60	3.79	2.57	85	0.13	85.9	2.09
90	4.50	2.78	95	0.15	82.5	1.89
180	6.48	3.37	100	0.24	81.2	1.82
360	9.43	4.36	100	0.28	80.0	1.75

*θ_{out} is the outlet temperature of fluid.

Table 2. The values of d, s, ℓ, w, θ_{out}, $\dot{E}$ of the model without S.T.C. (the upper table) and those of the model with S.T.C. (the lower table)

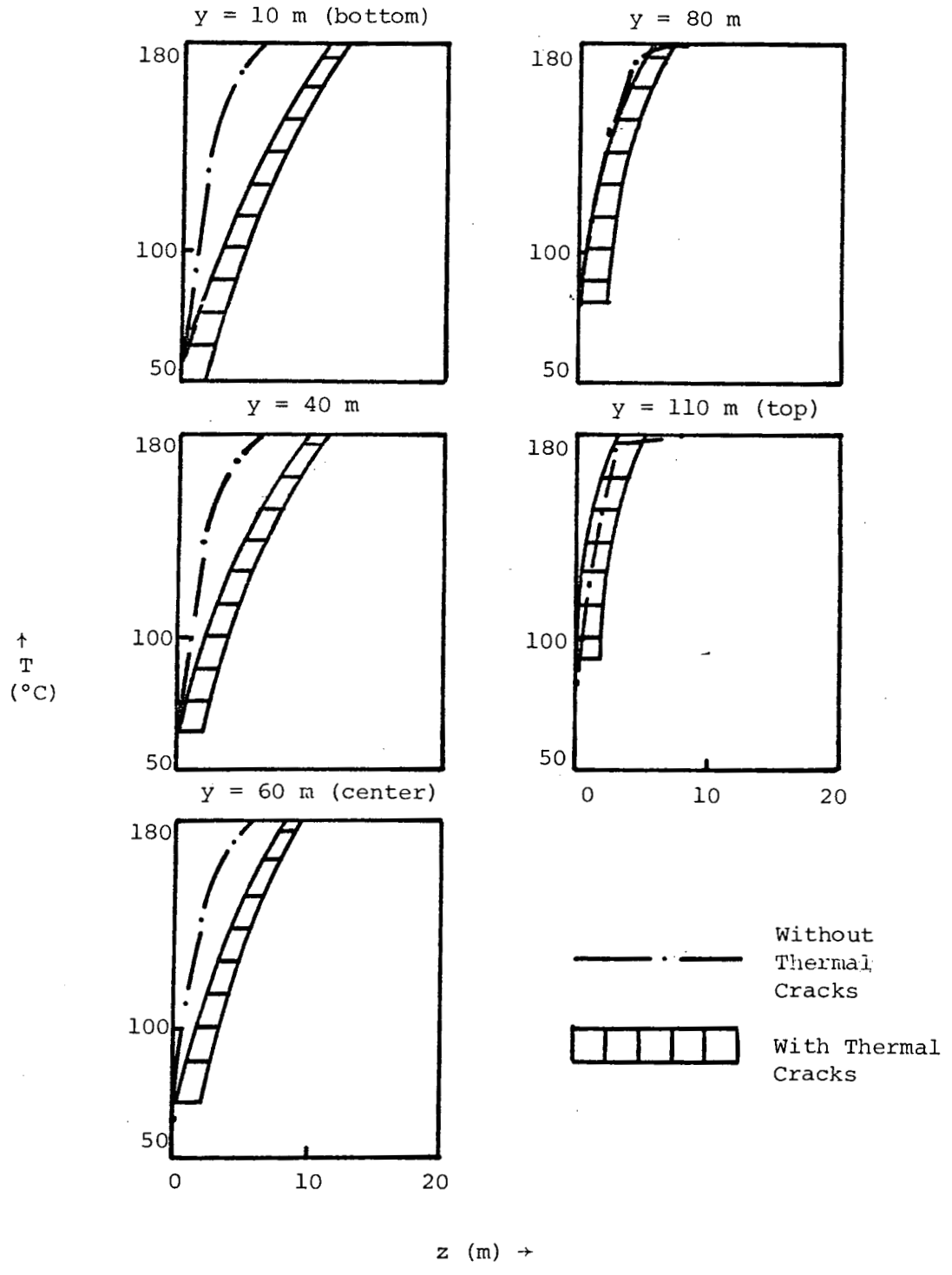

Figure 8. Temperature at x = 5 m, τ = 30 days for different y-coordinates

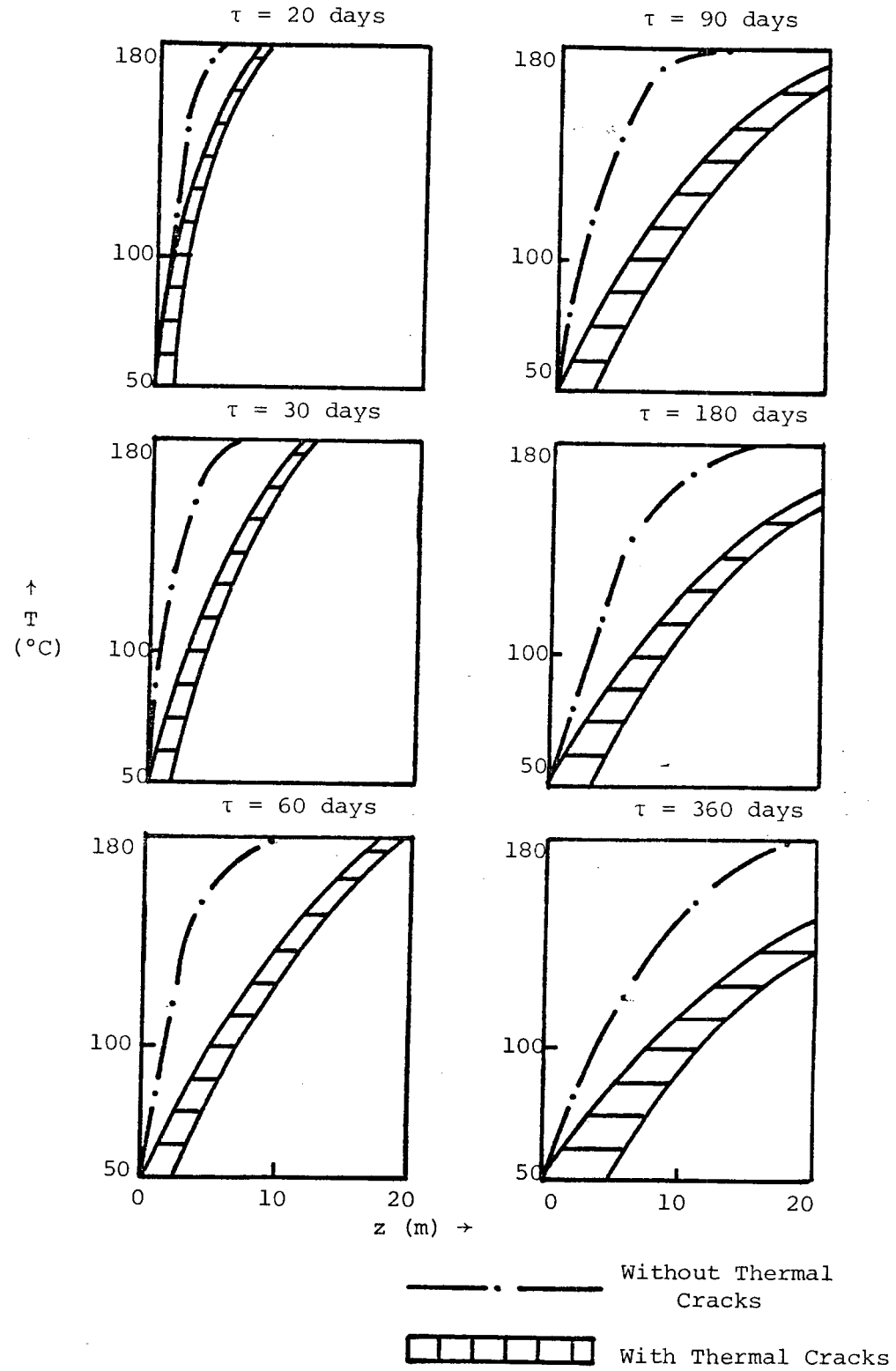

Figure 9. Temperature around the column at x = 5 m, y = 15 m for six time periods

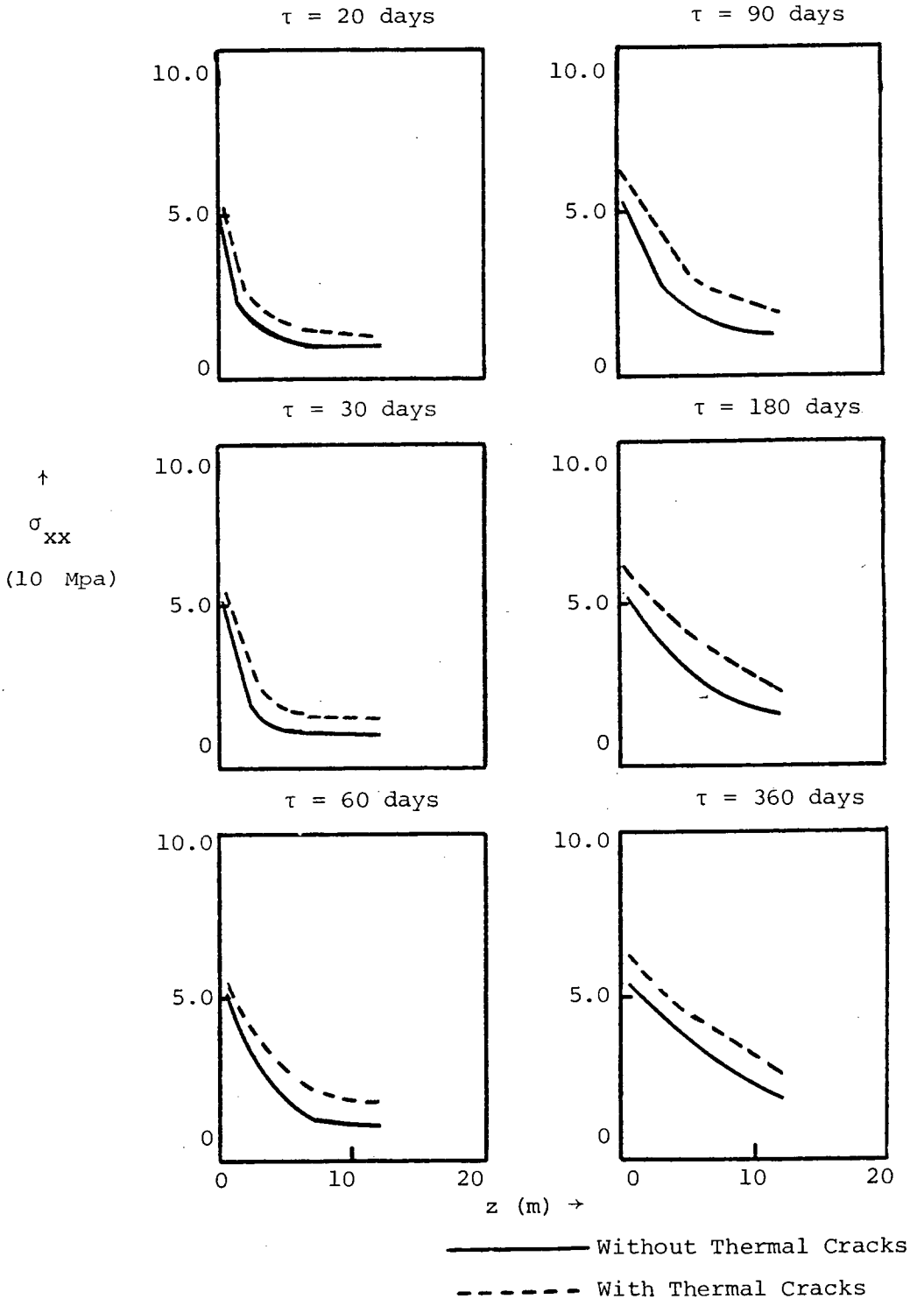

Figure 10. Thermal stress σ_{xx} around the column at x = 5 m, y = 15 m for six time periods

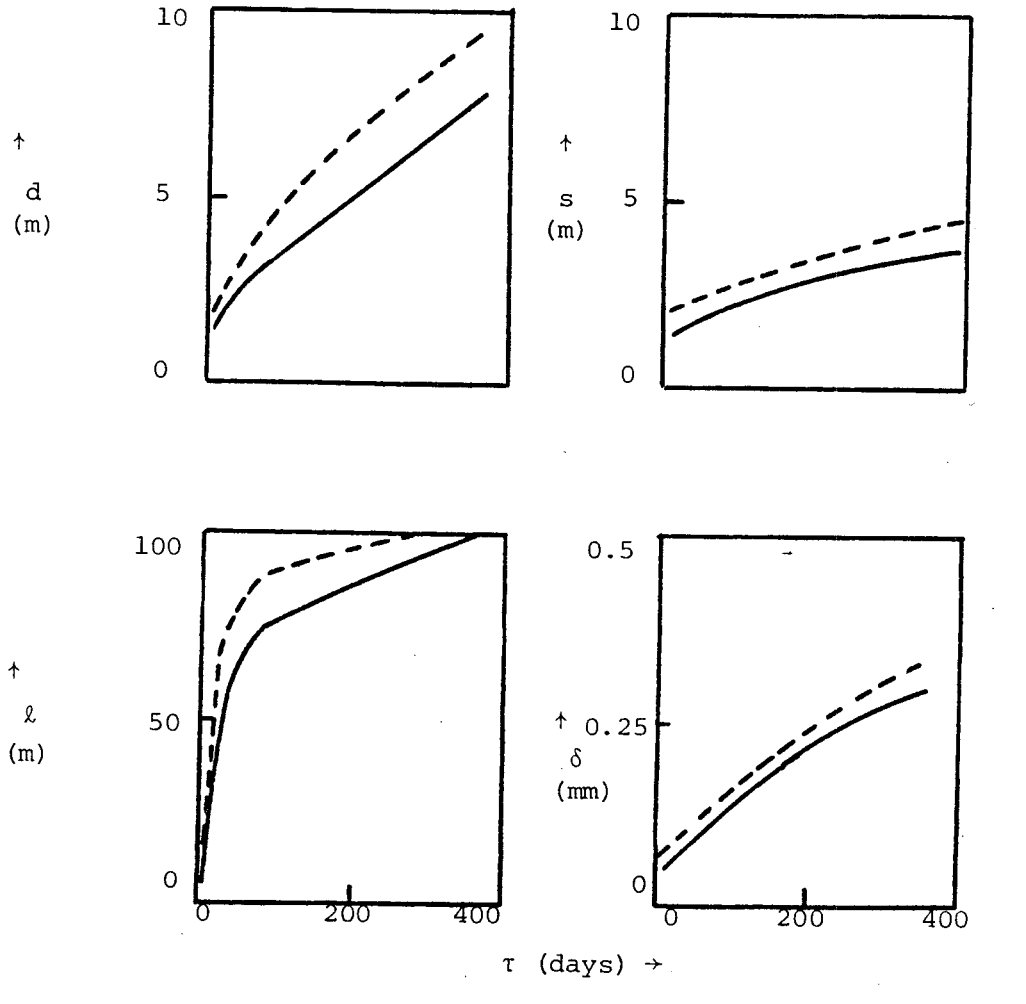

Figure 11. Depth (d), spacing (s), length (ℓ) and opening (w) of the reservoir for six time periods

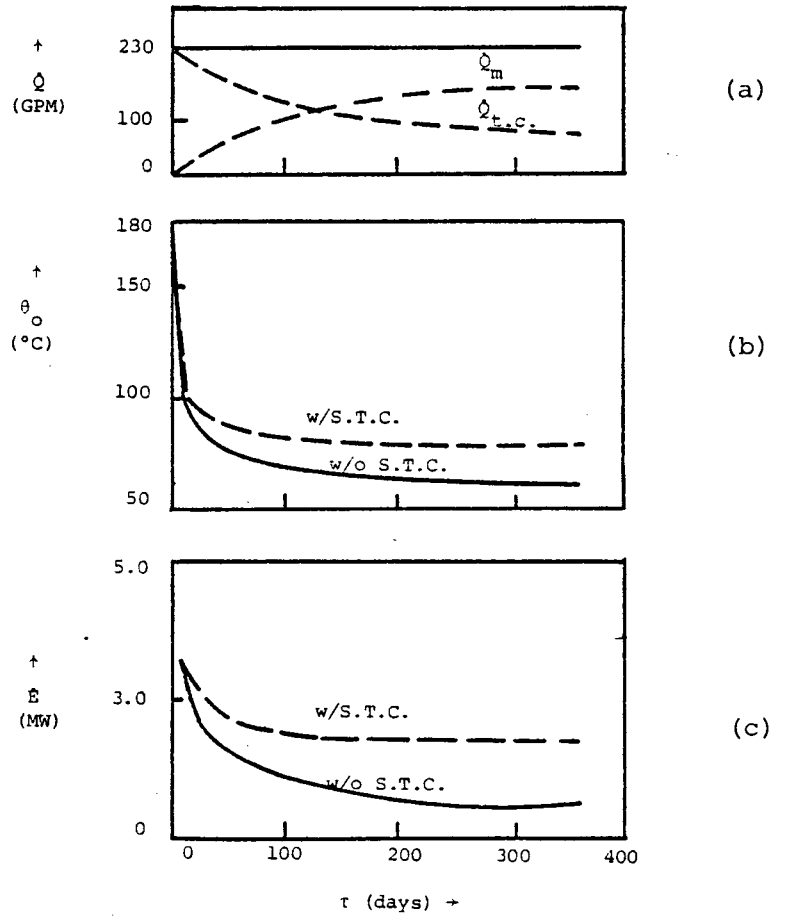

Figure 12.a. Water flow rate at the fracture midplane (y = 60 m). $\dot{Q}_m$ through the primary fracture, $\dot{Q}_{t.c.}$ through the thermal stress cracks

Figure 12.b. Reservoir coolant outlet temperature at a constant 50°C inlet temperature for an initial uniform rock temperature of 180°C

Figure 12.c. Reservoir thermal power

CHAPTER 6

CONCLUSIONS

1. Calculations are carried out for the LASL Fenton Hill HDR-Reservoir with H = 100 m, W = 70 m, t = 0.2 m, h = 2.6 km, $\dot{Q}$ = 230 gpm, θ_o = 50°C, T_r = 180°C, $\mu = 1.4 \times 10^{-4}$ Pa-sec and rock properties (see Table 1). Solutions can also be applied to the low-temperature-hot water reservoir.

2. Three equally-spaced edge cracks are initiated at ten days with d = 1.5 m, s = 1.34 m, w = 0.05 mm and ℓ = 5 m.

3. Rock temperature, in the presence of the circulating water of the secondary thermal cracks, is lower than the one in the absence of the secondary thermal cracks at various reservoir operation times (see Figure 9).

4. Thermal stress (σ_{xx}), in the presence of the circulating water of the secondary thermal cracks, is higher than the one in the absence of the secondary thermal cracks at various reservoir operation times (see Figure 10).

5. The geometry of the secondary thermal crack grows with time. The geometry in the presence of the circulating water of the thermal cracks is larger than the one in the absence of the circulating water of the thermal cracks.

6. For the small size main fracture system and with relatively low initial rock temperatures, the significant effect of thermal stress cracking is to flatten due to the temperature drawdown at later times. Even though the thermal power is more than doubled at 180 days, this occurs at an outlet reservoir temperature of only 81°C (see Figure 12). In Figure 12, at 60 days for a constant flow rate of 230 gpm, the thermal drawdown curve with thermal stress cracking is only about 12°C above that without thermal stress cracking (85.9 °C versus 73.5°C). It would appear that the effects of thermal stress cracking in this reservoir could easily be increased by several inadvertent shutdowns, changes in flow rate and by inferring a slightly larger effective heat transfer area for the reservoir.

7. Of investigation so far are effects of the circulating fluid (water) in the main hydraulic fracture and the resulting secondary thermal cracks on the temperature distribution and the resulting thermal stress field within the geothermal reservoir.

8. Neglecting the dynamic interaction between those growing secondary thermal cracks might cause reducing effect on temperature, thermal stress, and geometry of the rock. The real process, however, has to be studied by considering simultaneously the interacting effects of both circulating water and the growth of secondary thermal cracks.

REFERENCES

1. Hsu, Y. C., Lu. Y. M., Ju, F. D. and Dhingra, K. C., "Engineering Methods for Predicting Productivity and Longevity of Hot-Dry-Rock Geothermal Reservoir in the Presence of Thermal Cracks," Technical Completion Report NEMI15, New Mexico Energy Institute, P.O. Box 2E1, Las Cruces, New Mexico 88003 (1978).

2. Eskinazi, S., Principles of Fluid Mechanics, Allyn and Bacon, Inc., Boston, pp. 355-372 (1962).

3. Murphy, H. D., "Simplified Analysis of Temperature Distributions and Power Output of Hydraulically Fractured Geothermal Energy Reservoir," LASL, Los Alamos, private communication.

4. Bathe, K. J., Wilson, E. L., and Peterson, F. E., "SAP IV, A Structural Analysis Program for Static and Dynamic Response of Linear Systems," Report No. EERC 73-11, Earthquake Engineering Research Center, pp. IV.8.1-IV.8.19 (1973).

5. Lawton, R. G., "The AYER Heat Conduction Computer Program," LA-5613-MS, Los Alamos Scientific Laboratory, Los Alamos, New Mexico, 1974.